





**Geometrical-optics analysis of whispering-gallery modes in the layer of a coated spherical resonator**Gustav Schweiger , Thomas Weigel \*, and Andreas Ostendorf   
*Ruhr-University Bochum, Bochum, Germany* (Received 3 March 2020; revised 9 September 2020; accepted 12 October 2020; published 9 November 2020)

The resonance properties of a layer on the surface of a spherical microresonator are investigated using geometrical optics. The resonance condition for these shell-guided modes is formulated. Shell-guided modes are located in the layer and are bounded by the inner and outer surfaces of the layer. It is shown that the resonance condition depends—similarly to the case of a homogeneous resonator—on the difference of the phase propagation of a ray crossing the layer and the corresponding phase propagation along the associated caustic. It is shown that the layer can support resonances only in a certain thickness range that depends, among other factors, on the resonance order and the wave number. A straightforward explanation is given for these limitations. Comparison with solutions from wave theory shows excellent agreement. A simple analytical solution is presented to calculate the sensitivity of the resonator to the refractive index and the thickness of the layer as well as to the refractive index of the environment.

DOI: [10.1103/PhysRevA.102.053506](https://doi.org/10.1103/PhysRevA.102.053506)**I. INTRODUCTION**

Some interesting types among the numerous variants of optical microresonators are the coated microsphere and its near relative the hollow sphere. These types are especially important in sensing applications [1–10]. In most cases, wave theory is used for the theoretical description [2,7,8,11–19]. Sometimes perturbation theory is used to calculate the shift of the resonance wavelength as function of changes in the layer properties [1,2,20]. In biological applications, the resonator is often functionalized with a thin layer containing substances that bind selectively to molecules of the analyte [5,9,21]. Detailed descriptions of the state of the art and a comprehensive list of the corresponding literature can be found in recent reviews [22,23].

The layer serves various purposes. In biological applications and some chemical sensing applications, the layer should guarantee that the sensor interacts only with one particular biological or chemical agent. In other applications, e.g., for refractive index measurements, it was shown that the layer increases the sensitivity of the microresonators [3,13,15,24]. The possibility of compensating for thermal drift by coating a microsphere with a layer was also investigated [4,7]. The applicability of spherical resonators with a layer as chemical sensors was investigated [6,10,11]. Microscale hollow spheres have been used for force and pressure measurements [25,26].

In many reviews and research articles, dealing with resonances in microspheres, microrings, and other geometrical realizations of optical microresonators, the essence of a resonance is illustrated by geometrical optics. The reason is that the visual representation is clear, simple, and close to our imagination. In addition, the mathematical treatment is much simpler in geometrical optics than in wave theory. Wave the-

ory provides mathematical expressions for the resonator properties, while geometrical optics provides the explanations of the resonator's properties. This was the motivation to use geometrical optics for the work presented below. The drawback is that the geometrical-optics solutions are only approximate.

The standard picture is that a representative ray of the resonance circulates in a closed loop in the resonator, where the length of the loop is an integer multiple of the wavelength. However, quantitative theoretical treatments of resonances in optical microresonators by geometrical optics are scarce. This concept was used to calculate the effect of Goos-Hänchen shift on the mode spacing in a spherical cavity [18]. Formulas to calculate the resonance frequencies at grazing incidence were derived [27,28]. A less strict resonance condition for homogeneous spheres or cylinders was proposed [29]. It was shown that the resonant rays must not form closed loops, where the ray hits its tail after each round trip in phase. It is sufficient that the ray crosses its tail after each round trip in phase and the associated caustic is an integer multiple of the wavelength (plus  $\frac{1}{2}$  in the case of a sphere) [29–31]. In this model, a resonant ray fills the mode volume by its repeated round trips completely with radiation. There is no localized beam and therefore no Goos-Hänchen shift. In this picture, modes are confined by a reflecting surface, the outer boundary, and the caustic, the inner boundary. The caustic serves as a quasi-totally-reflecting surface with grazing incidence of the mode rays. Shell-guided modes are different. They are confined by two reflecting surfaces and the caustic is located beyond the mode. The mode volume is compressed into the layer and is narrower than an ordinary mode with the same mode number.

**II. RESONANCE CONDITION**

The following considerations will be restricted to the so-called whispering-gallery modes (WGMs). These are resonances where the angle of incidence exceeds the critical angle for total reflection. In addition, we consider only shell-guided

\*weigel@lat.rub.de

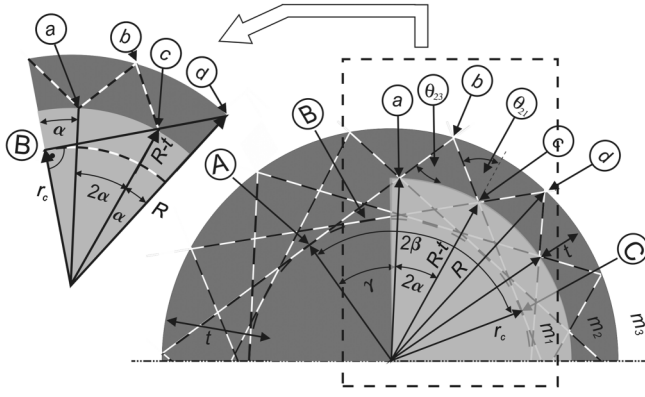


FIG. 1. Prominent rays of a homogeneous spherical resonator on the left, and a core-shell resonator on the right, with radius  $R$ , shell thickness  $t$ , and caustic radius  $r_c$ . The wavelength is symbolized by one black and white sequence, and  $m_i$  are the refractive indices of the core, shell, and surroundings.

modes: modes that are confined by the inner and outer boundaries of the shell. The situation is illustrated in Fig. 1. This figure shows typical rays of resonance modes located in a meridional cut through a spherical resonator. One sequence of white and black on the rays represents the wavelength. The left half of the cut in Fig. 1 shows rays of a resonance in a homogeneous spherical resonator. The resonance condition for such a mode reads [29,32]:

$$\begin{aligned} \Delta\Phi &= \Phi_{Abc} - \Phi_{ABC} = \frac{2\pi m_2}{\lambda} (2\overline{Ab} - r_c 2\beta) + \delta_{23} - \frac{\pi}{2} \\ &= 2\pi(n-1), \quad n = 1, 2, \dots \text{ and } r_c = \Lambda \frac{\lambda}{2\pi m_2}, \end{aligned} \quad (1)$$

where  $\Delta\Phi$  is the phase difference  $\Phi_{Abc}$  between a ray propagating from  $A$  via  $b$  to  $C$ , and the phase propagation  $\Phi_{ABC}$ , along the caustic from  $A$  via  $B$  to  $C$ . Here  $\lambda$  is the free space wavelength,  $m_i$  are the refractive indices (see Fig. 1),  $\delta_{23}$  is the phase change due to reflection on the shell surface (the  $m_2/m_3$  interface), and  $r_c$  is the caustic radius of the mode,  $\Lambda = \ell + \frac{1}{2}$ , with the mode number  $\ell$ :

$$\begin{aligned} \overline{AbC} &= \overline{Ab} + \overline{bC} = 2\sqrt{R^2 - r_c^2}, \quad \overline{ABC} = 2r_c \arccos \frac{r_c}{R}, \\ \delta_{23} &= -2 \arctan \left( N_{23}^2 \frac{\sqrt{m_2^2 \sin^2 \theta_{23} - m_3^2}}{m_2 \cos \theta_{23}} \right), \end{aligned} \quad (2)$$

$$N_{23} = \begin{cases} 1, & \text{TE mode,} \\ \frac{m_2}{m_3}, & \text{TM mode,} \end{cases} \quad m_2 > m_3, \quad \sin \theta_{23} = \frac{r_c}{R}.$$

We have used the formula for the phase shift for reflection on a plane interface, although relations for the phase shift on a curved interface are available [29,33,34]. It can be shown that the difference from the plane case is less than 3% in the cases investigated here [33]. Therefore, it seems to be well justified to use the formulas for total reflection on a plane interface.

The right side in Fig. 1 shows rays  $\overline{ab}$ ,  $\overline{bc}$ ,  $\overline{cd}$ , etc. of a shell-guided mode. This mode is bounded by the inner and outer surfaces of the layer. As shown in the figure, we assume that the resonator size,  $R$ , and the refractive index of the shell,  $m_2$ , are identical to those of the homogeneous resonator

shown on the left. The caustic of the shell-guided mode is located in the core of the resonator outside of the shell mode. The caustic on both sites in Fig. 1, both the mode of the homogeneous resonator and that of the shell-guided mode, may be identical. The rays of the shell-guided mode, which propagate in a zigzag way in the shell, from  $a$  over  $b$  to  $c$  etc. are virtual continuations of the rays in the homogeneous resonator in the corresponding outer region. That means, e.g., the phase propagation along  $\overline{ab}$  of the ray  $\overline{Ab}$  a member of homogeneous resonator is the same as along the ray  $\overline{ab}$  of the shell-guided mode. It satisfies, therefore, the resonance condition. In this case, the rays  $\overline{ab}$ ,  $\overline{bc}$ ,  $\overline{cd}$  also satisfy the resonance condition. That means, after each round trip each ray of the shell-guided mode crosses its tail in phase in the same way as the rays on the left of Fig. 1, belonging to the homogeneous resonator. Obviously, these rays satisfy the resonance condition. Continuations of the rays in the core region do not exist in the shell-guided mode. Therefore, they are shown in light gray. If the ray  $\overline{ab}$  is in phase with  $\overline{Aab}$ , the ray  $\overline{bc}$  is automatically in phase with  $\overline{bcC}$ . To manage that the ray  $\overline{cd}$  of the shell-guided mode is in phase with the ray  $\overline{Bcd}$  of the core mode, the reflection on the inner boundary of the shell has to be taken into account and the following condition has to be met:

$$\begin{aligned} \Phi_{Ab} + \delta_{23} + \Phi_{bc} + \delta_{21} &= \Phi_{AB} + \Phi_{Bc} + 2\pi(n-1), \\ n &= 1, 2, \dots \end{aligned} \quad (3)$$

As illustrated by the inset in Fig. 1 that shows a detail of the main figure indicated by the dashed line,  $\alpha = \arccos(\frac{r_c}{R}) - \arccos(\frac{r_c}{R-t})$  and one gets

$$\begin{aligned} \Phi_{Bc} &= \Phi_{Ab} - \Phi_{dc}, \quad \Phi_{dc} = \Phi_{bc}, \quad \Phi_{AB} = \frac{2\pi m_2}{\lambda} r_c 2\alpha \\ &= \frac{2\pi m_2}{\lambda} r_c \left( 2 \arccos \frac{r_c}{R} - 2 \arccos \frac{r_c}{R-t} \right), \\ \Phi_{bc} &= \sqrt{R^2 - r_c^2} - \sqrt{(R-t)^2 - r_c^2}. \end{aligned} \quad (4)$$

Combination of Eqs. (3) and (4) yields the phase difference of a ray traversing the mode volume, taking into account the phase shift due to reflections on the boundaries to the phase propagation along the associated arc on the caustic. In the case of resonance, the following condition for the phase difference must be satisfied:

$$\begin{aligned} \Delta\Phi &= \frac{2\pi m_2}{\lambda} 2 \left( \underbrace{\sqrt{R^2 - r_c^2} - \sqrt{(R-t)^2 - r_c^2}}_{\Delta\Phi_M} \right) + \underbrace{\delta_{23} + \delta_{21}}_{\Delta\Phi_R} \\ &\quad - \frac{2\pi m_2}{\lambda} r_c \left( 2 \arccos \frac{r_c}{R} - 2 \arccos \frac{r_c}{R-t} \right) \\ &= 2(n-1)\pi, \end{aligned} \quad (5)$$

$$\delta_{21} = 2 \arctan \left( N_{21}^2 \frac{\sqrt{m_2^2 \sin^2 \theta_{21} - m_1^2}}{m_2 \cos \theta_{21}} \right), \quad (6)$$

$$N_{21} = \begin{cases} 1, & \text{TE mode,} \\ \frac{m_2}{m_1}, & \text{TM mode,} \end{cases} \quad m_2 > m_1, \quad \sin \theta_{21} = \frac{r_c}{R-t}, \quad (7)$$

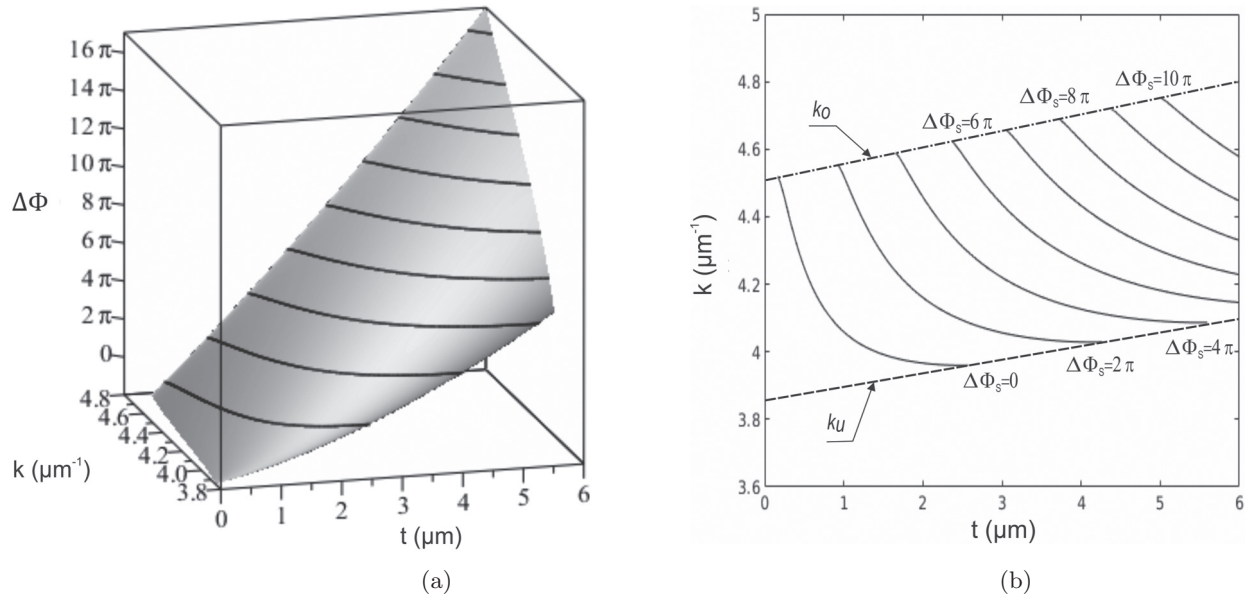


FIG. 2. Calculations for resonator radius  $R = 100 \mu\text{m}$ ,  $m_1 = 1.452$ ,  $m_2 = 1.7$ ,  $m_3 = 1.32$ , and  $\Lambda = 655.5$ . (a) Dependence of the phase function  $\Delta\phi$  on the wave number  $k$  and the layer thickness  $t$ ; contour lines at  $\Delta\phi = 0, 2\pi, 4\pi, \dots$ . (b) Dependence of the resonance mode wave number on the layer thickness for different resonance orders  $\Delta\phi = 0, 2\pi, 4\pi, \dots$ .

where  $\delta_{21}$  is the phase shift due to reflection on the core-shell interface, and  $\delta_{23}$  is the phase shift due to reflection on the outer shell interface. The phase equation (5) consists of three components: two volume-related terms  $\Delta\Phi_M$  and  $\Delta\Phi_C$  and one surface-related term  $\Delta\Phi_R$ . The first term  $\Delta\Phi_M$  represents the phase progression along a characteristic mode ray. This is a ray that propagates from one mode boundary to the opposite boundary and back, such as the ray  $M = abc$ .  $\Delta\Phi_R$  is the phase shift due to reflection on the outer and inner boundary of the layer, and  $\Delta\Phi_C$  is the phase accumulated along the arc  $C = 2\alpha r_c$ . Equation (5) states that the resonance condition is satisfied if the phase accumulated by a characteristic mode ray including the phase changes due to reflection on the boundaries is equal up to a multiple of  $2\pi$  to the phase accumulated along the associated arc on the caustic. In addition, in the case of a spherical resonator, the caustic radius  $r_c$  must satisfy the relation  $r_c = (\ell + \frac{1}{2})\frac{\lambda}{m}$ , where  $\ell$  is the mode number,  $\lambda$  the vacuum wavelength of the resonance, and  $m$  the refractive index in the mode region. The left side of Fig. 1 shows that in case of a mode in a homogeneous resonator the area between the caustic and the reflecting surface is completely filled with radiation. However, in the case of a shell-guided mode the radiation fills only the shell while the range between the caustic and the shell remains free of radiation. The radiation is compressed to the width of the shell.

### III. PROPERTIES OF SHELL-GUIDED RESONANCES

The properties of shell-guided TM modes were investigated using the following data set, unless otherwise specified:  $m_1 = 1.452$ ,  $m_2 = 1.7$ ,  $m_3 = 1.32$ ,  $R = 100 \mu\text{m}$ ,  $\Lambda = 666.5$ ,  $k = 4.5 \mu\text{m}^{-1}$ ,  $t = 0, \dots, 5 \mu\text{m}$ . The range of real solutions of the phase equation (2) with these parameters is shown in Fig. 2. Contour lines for  $\Delta\Phi = 0, 2\pi, 4\pi, \dots$  are also shown.

If the layer becomes small, the phase difference becomes negative. The reason is that the phase retardation caused by the supercritical reflections on the inner and outer boundaries of the layer is larger than the phase difference  $\Delta\Phi_M - \Delta\Phi_C$ . Resonances are not possible below this limit. The range of real phase differences has also a lower  $k_u$  and an upper limit in wave number  $k_o$ . The phase difference in Fig. 2 is calculated at a fixed mode number. Therefore, decreasing wave numbers mean increasing caustic radii  $r_c = \frac{\Lambda}{m_2 k}$ . The lower limit for  $k$  is reached if the inner boundary of the layer coincides with the caustic  $R - t = \frac{\Lambda}{m_2 k_u}$ . With increasing wave number  $k$ , the caustic radius  $r_c = \frac{\Lambda}{k m_2}$  decreases and the angle of incidence on the inner boundary decreases too; see Eq. (7).

Finally, if  $\theta_{21}$  is equal to the critical angle  $\sin \theta_{21} = \frac{m_1}{m_2} = \frac{r_c}{R-t} = \frac{\Lambda}{(R-t)m_2 k_o} \Rightarrow k_o = \frac{\Lambda}{m_1(R-t)}$ , the total reflection breaks down. The same holds for the reflection on the outer surface:  $\sin \theta_{23} = \frac{m_3}{m_2} = \frac{\Lambda}{m_2 k_M R} \Rightarrow k_M = \frac{\Lambda}{m_3 R}$ . Which surface determines  $k_o$  depends obviously on the ratios  $\frac{m_1}{m_3}$  and  $\frac{t}{R}$ . For wave numbers  $k > k_M$  there is no total reflection on the inner or outer boundary. The upper and lower limits of the range of real phase differences are shown in Fig. 2(a). In the case shown in Fig. 2, the reflection on the outer surface fails to be total at a layer thickness  $\frac{t}{R} > 0.09$  under the conditions investigated. If the total reflection breaks down on the outer boundary, the upper limit of  $k$  becomes independent of the layer thickness.

Comparisons of geometric optics results with wave theoretical calculations [3,13] are shown in Figs. 3(a) and 3(b). Only on the limits of the allowed layer thickness as given by geometrical optics, there are slight differences between the results of wave optics and geometrical optics. The differences on the limits are no surprise because in geometric optics the shell-guided resonances are strictly limited to the layer. The

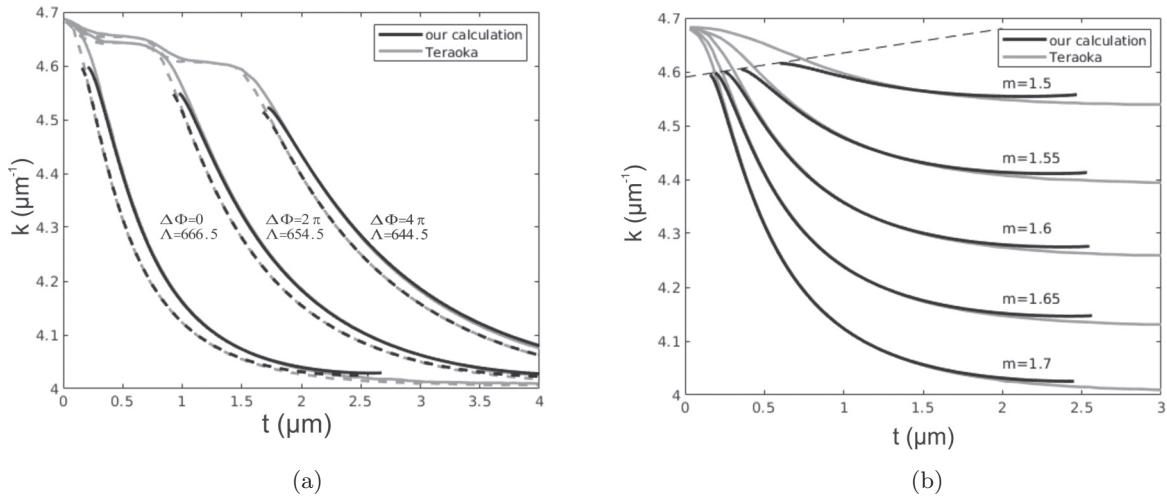


FIG. 3. Resonance wave number as function of the layer thickness. Comparison of geometrical-optics results with wave theory [3,13], gray lines. Same parameters as in Fig. 2 but for different resonance orders and mode numbers. (a) Effect of the mode order. (b) Effect of the refractive index of the layer (TM modes,  $\Lambda = 666.5$ ). Dashed lines indicate TE mode and solid lines TM modes.

boundaries of the layer are hard boundaries, which is not the case in wave theory. As the layer becomes thinner, wave theory provides a continuous transition from a resonator with a layer to a homogeneous resonator with the properties of the core. At the other end, with the layer becoming thicker, the resonator finally changes back into a homogeneous resonator, but with the properties of the layer.

There are no hard boundaries in wave theory. Part of the electromagnetic energy contained in the layer is always leaking into the surroundings, where the mode energy is exponentially decaying with increasing distance from the layer. As the layer becomes thinner the part of the mode energy outside the layer increases and surpasses finally that within the layer. This contradicts the assumption of geometrical optics that the mode energy is completely contained within the layer. Consequently, in geometrical optics no eigenmode is possible if the layer is so thin that a sizable part of the mode energy lies outside of the layer. This limitation appears clearly in Fig. 2. It shows that in the geometrical-optics solution shell-guided modes are restricted to a certain range of the thickness of the layer.

This range depends on the mode type and mode number and mode order. The wave-theoretical solutions show no such restriction. No restrictions on the location of the eigenmodes were made in the wave-theoretical calculations. The resonances at a layer thickness below the limit of geometrical optics are actually resonances that are partly located in the core. Resonances at a layer thickness above the geometrical-optics limit are actually shell resonances that only fill the layer to some extent. These resonances are not reflected on the inner boundary of the layer because the caustic radius, which is the inner limit of the mode, is larger than the radius of the inner boundary. There is no mode compression.

These modes have the same properties as modes of a homogeneous resonator with the same refractive index as the layer. There are a number of possibilities to use micro-optical resonators as sensors. In this investigation, the effects of changes in the size and refractive index of the layer and the refractive

index of the surrounding medium are investigated. In all cases shown, the radius  $R$ , the refractive index of the core,  $m_1$ , and of the surroundings,  $m_3$ , were kept constant. From the resonance condition analytical solutions for the sensitivities  $\frac{\partial k}{\partial t}$ ,  $\frac{\partial k}{\partial m_2}$ , and  $\frac{\partial k}{\partial m_3}$  can be found. The phase propagation along a ray is linearly proportional to  $km_2$  and the length of the ray, which in turn is linearly proportional to  $t$ . One would expect therefore that the dependences of the  $t$  sensitivity  $\frac{\partial k}{\partial t}$  on  $t$  and  $m_2$  are the same. However, the refractive index  $m_2$  changes the caustic radius and therefore the angle of incidence and so the length of  $M$  as well as that of the caustic arc  $K$ . The change of  $t$  has no effect on the caustic. The quantitative effects of  $t$  and  $m_2$  on  $\frac{\partial k}{\partial t}$  are therefore different. The sensitivity of shell-guided resonances on the refractive index of the layer is shown in Fig. 4.

It is interesting to see that the sensitivity increases with increasing layer thickness. This is also visible in Fig. 3(b).

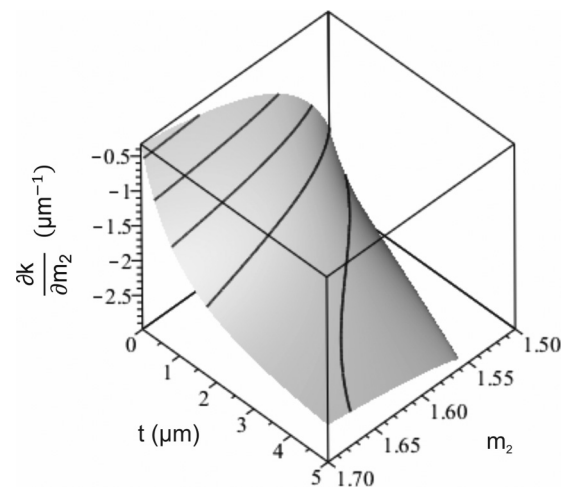


FIG. 4. Sensitivity of the resonant wave number  $k$  to the refractive index of the layer,  $m_2$ . All data are as before, with contour lines at  $\frac{\partial k}{\partial m_2} = -2.5, -2.0, \dots, -0.5 \mu\text{m}^{-1}$



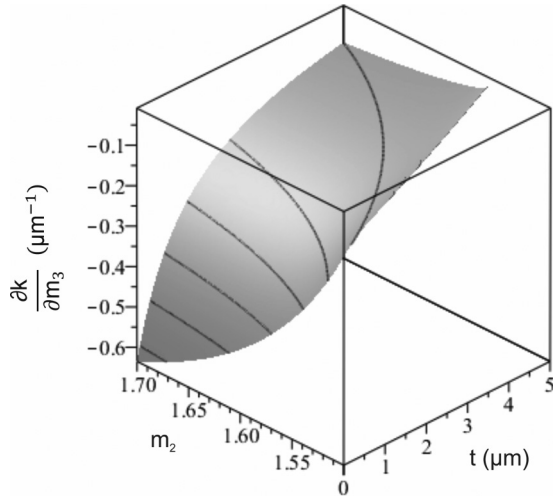


FIG. 5. Sensitivity of the resonant wave number  $k$  to the refractive index of the surroundings,  $m_3$ . Contour lines at  $\frac{\partial k}{\partial m_3} = -0.6, -0.5, \dots, -0.1 \mu\text{m}^{-1}$

The different behavior of the  $t$  sensitivity compared with the  $m_2$  sensitivity has its source in the dependence of the caustic radius on  $m_2$ . This dependence causes changes of the angle of incidence of the mode rays and that affects  $L$  as well as  $K$  and the phase shift due to reflection. As a result, the effect of the refractive index on the phase is larger than that of the wave number and increases with layer thickness. The growth rate of  $\frac{\partial \phi}{\partial m_2}$  increases with the layer thickness faster than  $\frac{\partial \phi}{\partial k}$ . This explains the dependence of the  $m_2$  sensitivity on  $t$  as shown in Fig. 4 as  $\frac{\partial k}{\partial m_2} = -\frac{\partial \phi}{\partial k} / \frac{\partial \phi}{\partial m_2}$ . Finally, the sensitivity of the layered resonator to changes of the external refractive index  $m_3$  also depends on the coating thickness. The external refractive index acts only on the phase shift due to reflection on the external boundary. The importance of this contribution to the phase shift of Eq. (7) becomes even more important the smaller  $\Delta\Phi_M$  and  $\Delta\Phi_K$  become. In effect, at  $t = 0$  these two terms disappear. The interaction of the optical properties of the surroundings with the resonator takes place at the location of reflection of a mode ray. The effect of this interaction depends on the dependence of the phase shift on the external refractive index but also on the number of reflections per round trip. The later increases as the layer becomes thinner. The sensitivities reproduced in Figs. 5, 4, and 6 hold for TM modes. Similar results can be found for TE modes. Examples are shown in Fig. 3(b).

#### IV. SUMMARY AND CONCLUSIONS

The theory of geometric optics was used to analyze the properties of shell-guided modes of a spherical resonator. These modes fill the width of the shell completely. They are bounded in the radial direction by two reflecting surfaces. Geometric optics was chosen because of its comparatively simple mathematical apparatus and its clarity. Geometric optics provides not only results for the resonance properties, but also explanations. The resonance condition for shell-guided modes was formulated. It was shown that shell-guided modes can only exist in a certain layer thickness range. The re-

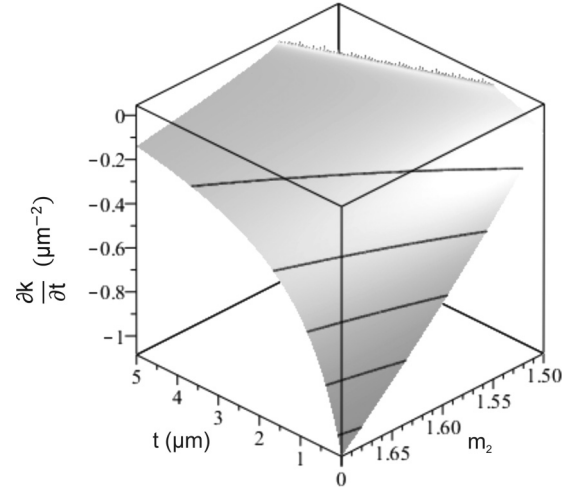


FIG. 6. Sensitivity of the resonant wave number  $k$  to the layer thickness  $t$ . Contour lines are at  $\frac{\partial k}{\partial t} = -1.0, -0.8, \dots, -0.2 \mu\text{m}^{-2}$ .

flections at the inner and outer boundaries cause a negative phase shift that must be compensated by the positive phase the beam accumulates as it passes through the layer. This requires a minimum layer thickness. The maximum thickness is reached when the inner boundary coincides with the caustic. By further increasing the thickness, the mode switches to the normal mode, which is limited by the caustic and a reflective surface. It no longer fills the whole cross section of the layer. The resonance condition was used to calculate the resonance wave numbers and their dependence on the thickness of the layer. A comparison with wave theory results shows an excellent agreement. The lower and upper limits of the resonance wave numbers were also investigated. A decrease in the wave number leads to an increase in the caustic radius. The limit is reached when the caustic radius coincides with the radius of the inner boundary of the layer. An increase in the resonance wave number reduces the caustic radius and thus the angle of incidence of the mode rays until the angle of incidence on the outer or inner surface falls below the critical angle for total reflection. Since only WG modes are considered, the angle of incidence on the reflective surfaces must be larger than the critical angle of incidence. Finally, the resonance condition was used to calculate the sensitivity of the resonance wave number to changes in the refractive index of the surrounding medium and to changes in the refractive index and thickness of the layer. It has been shown that a decrease in film thickness increases the sensitivity to changes in film thickness of the surrounding medium. The behavior of the sensitivity to changes in the refractive index of the layer is reversed; it decreases with decreasing layer thickness. In summary, the main effect of layer thickness on the properties of shell-guided modes is that a decrease in film thickness shifts the number of reflections on the surface relative to the length a beam travels within the resonator in favor of the reflections. Consequently, the effects of reflections on the resonance state increase. The resonator becomes more sensitive to the reflections and the refractive index of the environment. Conversely, an increase in thickness increases the influence of the resonator properties on the resonance condition and

the sensitivity to the refractive index of the layer. For sensor applications where the analyte affects the refractive index of the surrounding medium or the thickness of the layer, a thin layer with a high refractive index thick enough to support

shell-guided resonances would increase the sensitivity of the sensor. For sensor applications where the analyte only changes the refractive index of the resonator, the layer would not be advantageous.

- 
- [1] O. Gaathon, J. Culic-Viskota, M. Mihnev, I. Teraoka, and S. Arnold, Enhancing sensitivity of a whispering gallery mode biosensor by subwavelength confinement, *Appl. Phys. Lett.* **89**, 223901 (2006).
- [2] O. Gaathon, J. Culic-Viskota, M. Mihnev, I. Teraoka, and S. Arnold, Enhancing the sensitivity limit of the whispering gallery mode biosensor through sub-wavelength confinement of light, in *Proceedings of the 2007 Conference on Lasers & Electro-Optics/Quantum Electronics and Laser Science Conference (CLEO/QELS 2007)* (IEEE, Piscataway, NJ, 2007), Vols. 1–5, p. 925.
- [3] I. Teraoka and S. Arnold, Enhancing the sensitivity of a whispering-gallery mode microsphere sensor by a high-refractive-index surface layer, *J. Opt. Soc. Am. B* **23**, 1434 (2006).
- [4] M. Han and A. Wang, Temperature compensation of optical microresonators using a surface layer with negative thermo-optic coefficient, *Opt. Lett.* **32**, 1800 (2007).
- [5] S. Soria, F. Baldini, S. Berneschi, F. Cosi, A. Giannetti, G. N. Conti, S. Pelli, G. C. Righini, and B. Tiribilli, High- $q$  polymer-coated microspheres for immunosensing applications, *Opt. Express* **17**, 14694 (2009).
- [6] N. Lin, L. Jiang, S. M. Wang, L. Yuan, H. Xiao, Y. F. Lu, and H. L. Tsai, Ultrasensitive chemical sensors based on whispering gallery modes in a microsphere coated with zeolite, *Appl. Opt.* **49**, 6463 (2010).
- [7] N. Lin, L. Jiang, S. Wang, H. Xiao, Y. Lu, and H. Tsai, Thermostable refractive index sensors based on whispering gallery modes in a microsphere coated with poly(methyl methacrylate), *Appl. Opt.* **50**, 992 (2011).
- [8] N. Lin, L. Jiang, S. Wang, H. Xiao, Y. Lu, and H. Tsai, Ultrasensitive thermal sensors based on whispering gallery modes in a polymer core optical ring resonator, *Appl. Opt.* **50**, 6254 (2011).
- [9] C. E. Soteropulos, K. M. Zurick, M. T. Bernards, and H. K. Hunt, Tailoring the protein adsorption properties of whispering gallery mode optical biosensors, *Langmuir* **28**, 15743 (2012).
- [10] M. Eryurek, Y. Karadag, N. Tasaltin, N. Kilinc, and A. Kiraz, Optical sensor for hydrogen gas based on a palladium-coated polymer microresonator, *Sens. Actuat. B* **212**, 78 (2015).
- [11] R. L. Hightower and C. B. Richardson, Resonant Mie scattering from a layered sphere, *Appl. Opt.* **27**, 4850 (1988).
- [12] I. Teraoka, S. Arnold, and F. Vollmer, Perturbation approach to resonance shifts of whispering-gallery modes in a dielectric microsphere as a probe of a surrounding medium, *J. Opt. Soc. Am. B* **20**, 1937 (2003).
- [13] I. Teraoka and S. Arnold, Whispering-gallery modes in a microsphere coated with a high-refractive index layer: polarization-dependent sensitivity enhancement of the resonance-shift and TE-TM resonance matching, *J. Opt. Soc. Am. B* **24**, 653 (2007).
- [14] I. Teraoka and S. Arnold, Variational principle in whispering gallery mode sensor responses, *J. Opt. Soc. Am. B* **25**, 1038 (2008).
- [15] N. Lin, L. Jiang, S. Wang, Q. Chen, H. Xiao, Y. Lu, and H. Tsai, Simulation and optimization of polymer-coated microsphere resonators in chemical vapor sensing, *Appl. Opt.* **50**, 5465 (2011).
- [16] D. Ristic, A. Chiappini, M. Mazzola, D. Farnesi, G. Nunzi-Conti, G. C. Righini, P. Feron, G. Cibiel, M. Ferrari, and M. Ivanda, Whispering gallery mode profiles in a coated microsphere, *Eur. Phys. J. Spec. Top.* **223**, 1959 (2014).
- [17] Y. A. Demchenko and M. L. Gorodetsky, The effect of an absorbed layer on the resonant frequencies and  $q$ -factors of spherical microresonators, *Moscow Univ. Phys. Bull.* **70**, 195 (2015).
- [18] D. Q. Chowdhury, D. H. Leach, and R. K. Chang, Effect of the Goos-Hänchen shift on the geometrical-optics model for spherical-cavity mode spacing, *J. Opt. Soc. Am. A* **11**, 1110 (1994).
- [19] T. Kaiser, S. Lange, and G. Schweiger, Structural resonances in a coated sphere: investigation of the volume-averaged source function and resonance positions, *Appl. Opt.* **33**, 7789 (1994).
- [20] S. Arnold and O. Gaathon, Spectroscopy of photonic atoms: A means for ultra-sensitive specific sensing of bio-molecules, in *Advances in Spectroscopy for Lasers and Sensing*, edited by B. Di Bartolo and O. Forte (Springer, Dordrecht, 2006), pp. 1–18.
- [21] S. Soria, F. Baldini, S. Berneschi, M. Brenci, F. Cosi, A. Giannetti, G. N. Conti, S. Pelli, G. C. Righini, and B. Tiribilli, Polymer-functionalised microspheres for immunosensing applications, in *Optical Fibers and Sensors for Medical Diagnostics and Treatment Applications X*, edited by I. Gannot, Proceedings of SPIE, Vol. 7559 (SPIE, Bellingham, WA, 2010).
- [22] G. C. Righini and S. Soria, Biosensing by WGM microspherical resonators, *Sensors* **16**, 905 (2016).
- [23] G. N. Conti, S. Berneschi, and S. Soria, Aptasensors based on whispering gallery mode resonators, *Biosensors* **6**, 28 (2016).
- [24] N. Lin, L. Jiang, S. M. Wang, H. Xiao, Y. F. Lu, and H. L. Tsai, Design and optimization of liquid core optical ring resonator for refractive index sensing, *Appl. Opt.* **50**, 3615 (2011).
- [25] T. Ioppolo, M. I. Kozhevnikov, V. Stepaniuk, M. V. Otugen, and V. Sheverev, Micro-optical force sensor concept based on whispering gallery mode resonators, *Appl. Opt.* **47**, 3009 (2008).
- [26] T. Ioppolo and M. V. Otugen, Pressure tuning of whispering gallery mode resonators, *J. Opt. Soc. Am. B* **24**, 2721 (2007).
- [27] M. L. Gorodetsky and A. E. Fomin, Geometrical theory of whispering-gallery modes, *IEEE J. Sel. Top. Quantum Electron.* **12**, 33 (2006).
- [28] T. Ioppolo, N. Das, and M. V. Ötügen, Whispering gallery modes of microspheres in the presence of a changing surrounding medium: A new ray-tracing analysis and sensor experiment, *J. Appl. Phys.* **107**, 103105 (2010).

- [29] G. Roll and G. Schweiger, Geometrical optics model of mie resonances, *J. Opt. Soc. Am. A* **17**, 1301 (2000).
- [30] G. Roll and G. Schweiger, Resonance shift of obliquely illuminated dielectric cylinders: Geometrical-optics estimates, *Appl. Opt.* **37**, 5628 (1998).
- [31] G. Roll, T. Kaiser, and G. Schweiger, Eigenmodes of spherical dielectric cavities: coupling of internal and external rays, *J. Opt. Soc. Am. A* **16**, 882 (1999).
- [32] G. Schweiger and M. Horn, Effect of changes in size and index of refraction on the resonance wavelength of microspheres, *J. Opt. Soc. Am. B* **23**, 212 (2006).
- [33] J. Schulte and G. Schweiger, Resonant inelastic scattering by use of geometrical optics, *J. Opt. Soc. Am. A* **20**, 317 (2003).
- [34] A. W. Snyder and J. D. Love, Reflection at a curved dielectric interface – electromagnetic tunneling, *IEEE Trans. Microw. Theor. Tech.* **23**, 134 (1975).